1960

Analysis and simulation of a cross-correlation communication system

Dennis Jay Gooding

Department:

ANALYSIS AND SIMULATION OF A CROSS-CORRELATION COMMUNICATION SYSTEM

BY

DENNIS JAY GOODING

A

THESIS

submitted to the faculty of the

SCHOOL OF MINES AND METALLURGY OF THE UNIVERSITY OF MISSOURI

in partial fulfillment of the work required for the

Degree of

MASTER OF SCIENCE IN ELECTRICAL ENGINEERING

Rolla, Missouri

1960

Approved by

Roger E. Nolte (advisor) C. A. Johnson

Ralph E. Lee

TABLE OF CONTENTS

LIST OF TABLES

LIST OF FIGURES

FIGURE PAGE

LIST OF SYMBOLS

T -- duration of a transmitted symbol.

$s(t)$ -- waveform of a transmitted symbol.

$h(t)$ -- waveform of the interfering noise.

$g(t)$ -- received signal waveform.

$s_k(t)$ -- wave form of the K-th symbol.

$p(s_k)$ -- a posteriori probability that the K-th symbol was transmitted.

exp -- exponential function.

S_i -- mean signal power per cycle bandwidth.

N_i -- mean noise power per cycle bandwidth.

W -- total bandwidth of signal.

θ -- interval of Fourier expansion of $g(t)$ and $s(t)$.

a_i -- i-th Fourier coefficient of the expansion of $s(t)$.

b_i -- i-th Fourier coefficient of the expansion of $h(t)$.

ϕ_i -- phase of the i-th component of the Fourier expansion of $s(t)$.

ψ_i -- phase of the i-th component of the Fourier expansion of $h(t)$.

ω -- radian frequency

ω_i -- the frequency of the i-th Fourier component.

$S(\omega)$ -- smoothed power spectrum of the signal $s(t)$.

$N(\omega)$ --- smoothed power spectrum of the noise $h(t)$.

$i(t)$ -- impulse response of the integrator.

$I(\omega)$ -- transfer function of the integrator.

$H(\omega)$ -- squared magnitude of the channel filter transfer function.

W_i -- effective bandwidth of the integrator radians/sec.

S_{o1} -- average output signal power of integrator containing signal.

N_{o1} -- average noise component of output power of integrator containing signal.

N_{o2} -- average noise output power of integrator not containing signal

X_1 -- total output voltage at the sample time of the integrator containing signal.

X_2 -- total output voltage at the sample time of the integrator not containing signal.

P_e -- probability of error per bit.

CHAPTER I

INTRODUCTION

In the past decade, a number of important advancements were made in the field of communication systems. Notable among these was the development of the cross-correlation detection technique for detecting signals in high-interference-level environments.

I. THE PROBLEM

Statement of the problem. The purpose of this study was (1) to calculate the probability of error as a function of receiver input signal-to-noise ratio for a typical communication system employing cross-correlation detection; (2) to design and construct an experimental model of such a communication system for the purposes of demonstrating the operation of the system and verifying the theoretical calculations.

Importance of the study. There exist many instances where communication must be maintained under conditions of low signal to noise ratio. For example, in space satellites and in rockets for space exploration, weight and power supply limitations often restrict the output power of the

radio transmitters. Furthermore, the difficulty involved in maintaining accurate spatial orientation with respect to the receiver on Earth precludes the use of high-gain antennas in most cases.

In these instances, and in many others where the signal-to-noise ratio at the receiver is small, it may be necessary to employ some of the more sophisticated detection techniques, such as cross correlation detection.

II. SCOPE OF THE INVESTIGATION

The investigation conducted was composed of two parts, a theoretical investigation and an experimental investigation.

Theoretical investigation. A cross-correlation detection system was analyzed to determine the probability of error as a function of receiver input signal-to-noise ratio. The effects of time desynchronization and frequency desynchronization of the receiver, relative to the transmitter, was not considered. Although numerical values of probability of error were calculated for one specific set of system constants, equations were developed from which the probabilities of error corresponding to other sets of system constants may also be calculated.

Experimental Investigation. A simplified model of a cross-correlation detection system was designed and built. Experiments were conducted to determine the probability of error for various values of received signal-to-noise ratio.

III. ORGANIZATION OF REMAINDER OF THESIS

In Chapter II the history of the use of cross-correlation in communication is traced. The contributions of some of the more important workers in the field are acknowledged. An introduction to cross-correlation detection is presented in Chapter III. Through investigation of a mathematical model of a data communication system, it is shown that cross-correlation is an optimum detection process. The relationship between the cross-correlation detector and the mathematical operation of cross-correlation is discussed. Equations are derived in Chapter IV for the output signal and noise powers of a particular cross-correlation detector. These equations are then used to determine the probability of error of the system as a function of input signal-to-noise ratio. The design of the experimental equipment is discussed in Chapter V, and each of the major components of the system is considered separately. In Chapter VI the experimental investigation is described. An outline of the procedure used and the

results obtained is presented. The final chapter, Chapter VII, contains the conclusions drawn from the theoretical and experimental work.

CHAPTER II

REVIEW OF THE LITERATURE

The first publication concerning the application of correlation functions to the detection of signals in noise is due to Lee, Cheatham, and Wiesner.[1] They compared the effectiveness of the cross-correlation and the autocorrelation operations in detecting the presence of periodic signals buried in noise. Fano[2] investigated a detection system which was similar to a cross-correlation detector, except that it employed a low pass filter in place of an integrator. Fano, like Lee, Cheatham, and Wiesner, was concerned with detecting the presence of a periodic signal in noise rather than applying the detector to a communication system.

In the course of their work on statistical detection theory Woodward and Davies[3] showed that cross-correlation detection is an optimum decision process in the sense that it maximizes the likelihood of a correct decision when the signal is disturbed by additive Gaussian noise.

Green[4] derived expressions for the output signal-to noise ratio of two types of correlation detector for very

---

[1]All references are in the bibliography

general input conditions. Much of the derivation of output signal-to-noise ratio performed in Chapter IV is based on work done by Green.

In addition to the references cited, considerable work of a classified nature has been performed, especially by the staff of the Massachusetts Institute of Technology Lincoln Laboratories.

CHAPTER III

THEORY OF CROSS-CORRELATION DETECTION

A brief outline of the theory and mathematical justification of cross-correlation detection is here presented.

I. DERIVATION OF CROSS-CORRELATION AS AN IDEAL DETECTION SYSTEM

The logical model shown in Figure 1 is representative of the operation of a large class of communication systems in which discrete, rather than continuous information is transmitted.

Transmitter. In this model, the digital input data determine which of the n possible signals will be transmitted at any time. Each signal, when selected, is transmitted for a time duration T. At the end of this period another selection is made according to the new st of the input data. The output of the transmitter consis of a sequence of signals, each of duration T. These sig of duration T will be referred to as symbols in the ensu work.

Communication channel. The communication channel

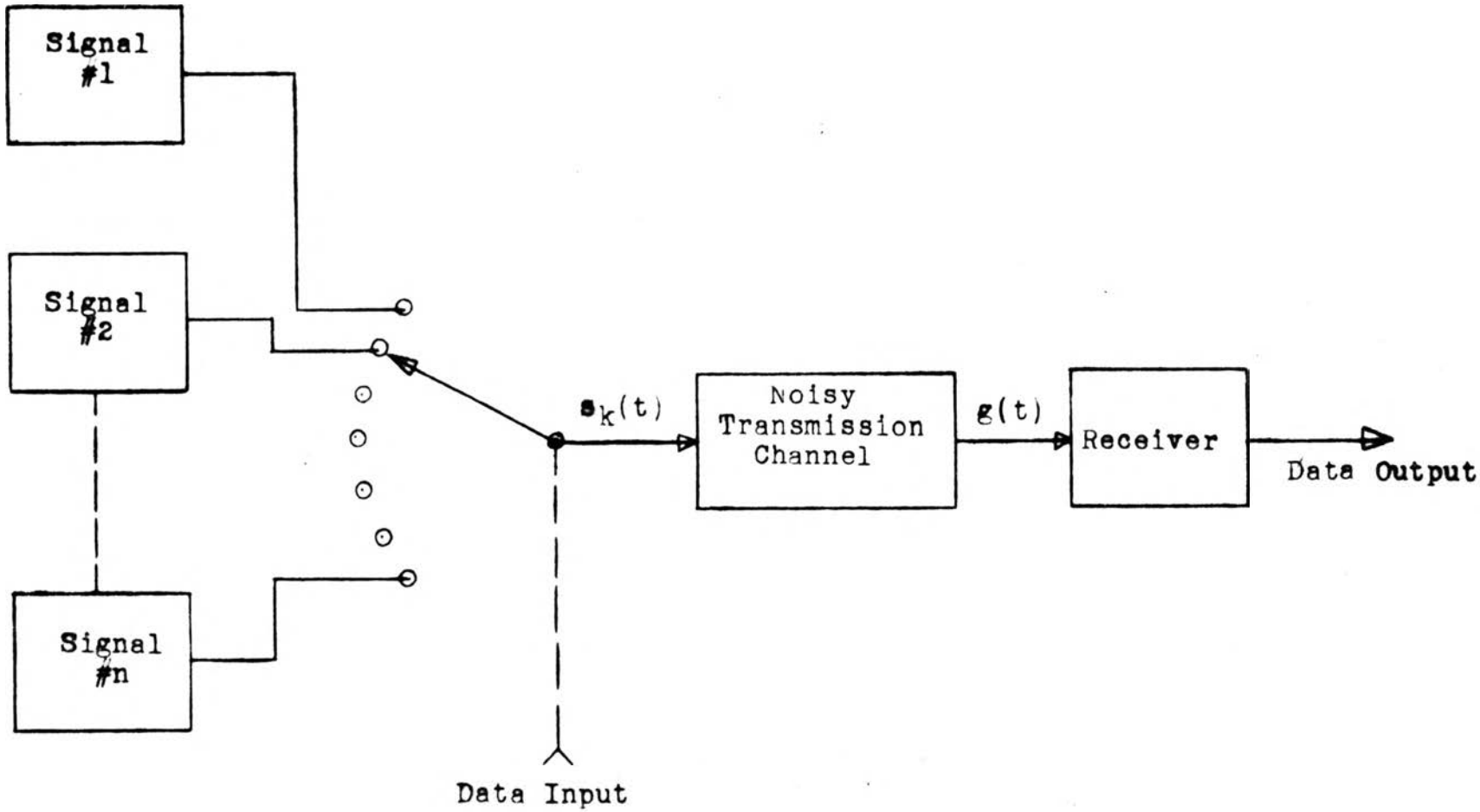

FIGURE 1

BLOCK DIAGRAM OF A GENERAL DIGITAL-DATA COMMUNICATION SYSTEM

may be a radio channel, a telephone line, or other transmission medium. In passing through the communication channel some distortion of the transmitted symbols ordinarily results. Consequently, the received symbols differ somewhat from the transmitted symbols. In many communication channels the distortion consists mainly of random noise (usually assumed to be Gaussian) linearly added to the signal. For purposes of analysis, receiver noise is usually considered to be a portion of the channel noise.

Receiver. The purpose of the receiver is to determine, on the basis of the received signal, which symbol was most probably intended during any given interval T. The effect of noise in the received signal is to cause uncertainty to exist at the receiver as to the identity of the various received symbols. As a consequence, the receiver will make incorrect decisions (errors) with a probability determined by the relative energy of the symbols and the noise.

The ideal receiver. An ideal receiver may be defined as a receiver which minimizes the probability of error for a given input condition. Assume the existence of an ideal receiver. Assume further that upon receipt of a distorted

symbol the ideal receiver computes the a posteriori probabilities $p(s_k)$ that the k-th symbol was intended. And, that upon determining all n of these probabilities, it selects that symbol corresponding to the largest of the $p(s_k)$. Woodward and Davies[3] have shown that for the case where the noise has a Gaussian amplitude distribution, the a posteriori probability that the k-th signal was the one sent is given by

$$P(s_k) = A \exp\left\{ -\frac{1}{N_i} \int_T \left[g(t) - s_k(t) \right]^2 dt \right\} \qquad (1)$$

Here, A is a constant chosen to normalize $p(s_k)$; N_i is the noise power per unit bandwidth; $g(t)$ is the received symbol; and $s_k(t)$ is the k-th symbol. The integration is over the duration of a symbol. It has been assumed in the above that the n symbols are transmitted with equal a priori probabilities. The symbol $s_k(t)$ which maximizes $p(s_k)$ is the one which minimizes the integral

$$\int_T \left[g(t) - s_k(t) \right]^2 dt$$

or its equivalent,

$$\int_T \left[g^2(t) - 2\, g(t)\, s_k(t) + s_k^2(t) \right] dt$$

If all symbols have the same average power, minimization of the above integral corresponds to the maximization of

$$\int_T g(t)\, s_k(t)\, dt$$

Cross-correlation detector. The last-mentioned operation is one which can be performed physically, and a detector which performs the indicated operation is called a cross-correlation detector. In summary, the operation of a cross-correlation detector is as follows:

1. The received symbol waveform, g(t), is multiplied by locally-generated copies of each of the n possible symbols, $s_k(t)$. These locally-generated symbols are referred to as reference symbols.
2. Each of the products above are integrated over a symbol duration.
3. The magnitudes of the various integrals are compared at the end of the integration period, and the largest magnitude is selected as being indicative of the most probably correct symbol.

Precise synchronization of the received symbols with the various locally-generated symbols is implied in Equation 1. That is, the signal component of g(t) is synchronous with one of the n reference symbols at any given time.

Practical receivers require some means of establishing and maintaining this synchronization. In the following work it is assumed that exact synchronization is present.

It is apparent that approximate orthogonality of the various symbols $s_k(t)$ is desirable, since this condition would result in the greatest exaltation of the $p(s_k)$ which corresponds to the correct symbol.

II. RELATIONSHIP OF THE CROSS-CORRELATION DETECTOR TO THE CROSS-CORRELATION FUNCTION

The cross-correlation function of two variates $f_1(t)$ and $f_2(t)$ is defined as[5]

$$\phi_{12}(\tau) = \lim_{T \to \infty} \frac{1}{2T} \int_{-T}^{T} f_1(t)\, f_2(t+\tau)\, dt \qquad (2)$$

It is seen to be a function of the time displacement between the two variates. In statistical work it is used as a measure of the linear dependence of two variates (not necessarily time functions) as a function of their relative displacement .

For the case where the functions $f_1(t)$ and $f_2(t)$ are of finite total energy, $\phi_{12}(\tau) = 0$. In order to deal with functions of this type, a slightly different form of the cross-correlation function is defined. It is known as the

finite cross-correlation function, and is written

$$\psi(\tau) = \int_{-\infty}^{\infty} f_1(t)\, f_2(t+\tau)\, dt \qquad (3)$$

The cross-correlation detector is so named because its operation is based on calculating the finite cross-correlation $\psi(0)$ of the input signal with each of the reference symbols.

CHAPTER IV

ANALYSIS OF A CROSS-CORRELATION COMMUNICATION SYSTEM

A mathematical analysis of a typical communication system employing cross-correlation detection is performed to determine the probability of error as a function of receiver input signal-to-noise ratio.

I. SPECIFICATION OF THE SYSTEM

The system analyzed is a binary data transmission system employing cross-correlation detection. Figure 2 shows a block diagram of the system. One of two symbols is selected during a bit interval T according to whether that bit is a MARK or SPACE (one or zero). This corresponds to the general system of Chapter III in which n is two. The MARK and SPACE symbols consist of samples of duration T drawn from two statistically independent Gaussian noise sources.

At the receiver identical copies of the MARK and SPACE symbols are generated in exact phase with the transmitter symbols. For each symbol transmitted, the receiver performs a cross-correlation of the received symbol with each of the two locally-generated symbols, and selects the

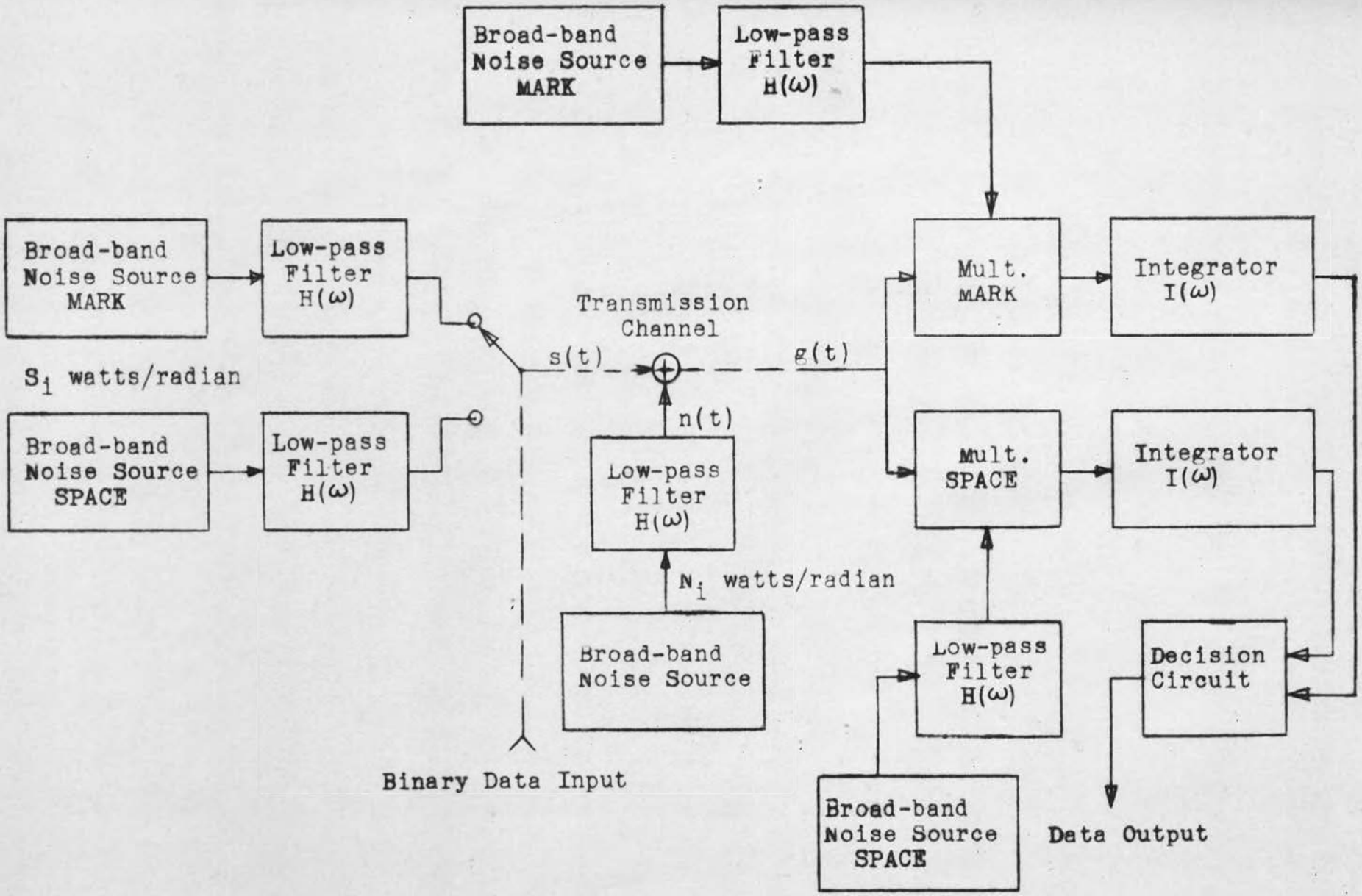

FIGURE 2

BLOCK DIAGRAM OF A CROSS-CORRELATION COMMUNICATION SYSTEM

symbol yielding the larger correlation.

The following definitions and assumptions are used throughout the present chapter:

1. The transmission medium is linear, stationary, and non-dispersive. It is corrupted by additive Gaussian noise generated by passing white noise of power density N_i watts per radian through a low-pass filter whose power transfer function is $H(\omega)$.
2. The signals are independent, ergodic functions of time having Gaussian amplitude distributions and zero mean. They are generated by passing white noise with power density S_i watts per radian through a low-pass filter whose power transfer function is $H(\omega)$.
3. All components of the receiver have a sufficient dynamic range that linear operation is assured.
4. Low-pass operation is used. That is, there can be no frequency or phase desynchronization between the received signal and the locally-generated reference signals.
5. It is assumed that no time desynchronization exists between the received symbol and the reference symbols.

6. The low-pass filters employed in generating the signals and noise are 3-pole, 1-decibel-ripple, low-pass Chebyshev filters having a tolerance bandwidth of 5 kc.
7. The multipliers are assumed to be ideal four-quadrant analog multipliers.
8. The integrators are assumed to be ideal. Their output is sampled at the end of each symbol interval (33.3 msec.), and the integrator is reset to zero.

II. CALCULATION OF THE OUTPUT SIGNAL-TO-NOISE RATIO

Procedure. For purposes of analysis, it is assumed that a MARK signal has been transmitted for a symbol duration T, and that the receiver has performed a cross-correlation of the received signal with each of the two reference signals. If, then, at the end of the symbol interval the output of the MARK integrator is greater than the output of the SPACE integrator a correct decision will occur.

The signal and noise powers at the output of the MARK integrator may be calculated by a method similar to that employed by Green[4]. The calculations are performed as follows.

The transmitted signal s(t) and the interfering noise n(t) are each considered to be members of an associated infinite ensemble of random functions each of duration Θ. s(t) and n(t) are expanded in Fourier series in the interval Θ to obtain two line spectra. The resulting line spectrum at the output of the multiplier is next calculated. Finally, the output spectrum of the multiplier is multiplied by the square of the magnitude of the transfer function of the integrator to yield the line spectrum of the integrator output. The interval Θ is allowed to become infinite in such a manner that the line spectra become continuous functions of frequency. The summations of Fourier coefficients become integrals involving the power spectra of s(t) and n(t). The signal component of the integrator output is the dc term of the output spectrum, while the terms at higher frequencies represent fluctuation or noise in the output.

Calculations. Employing the representation of Rice[6], the various input waveforms may be written

$$s(t) = \sum_{i=1}^{\Theta W} a_i \cos(\omega_i t + \phi_i) \tag{4}$$

$$n(t) = \sum_{i=1}^{\Theta W} b_i \cos(\omega_i t + \gamma_i) \tag{5}$$

$$g(t) = s(t) + n(t) = \sum_{i=1}^{\Theta W} [a_i \cos(\omega_i t + \phi_i) + b_i \cos(\omega_i t + \gamma_i)] \tag{6}$$

where ϕ_i and γ_i are uniformly distributed in the interval 0 to 2π, and $\Delta\omega \equiv (\omega_{i+1} - \omega_i) = \frac{2\pi}{\Theta}$.

W is a bandwidth sufficiently large to encompass all significant frequency components of s(t) and n(t). In the above Θ is much greater than the symbol duration T. At a suitable point in the analysis Θ is allowed to become infinite in such a way that $\Delta\omega$ approaches zero. The validity of the above expansion is evident when it is recalled that by the "sampling theorem" a time function of duration Θ and approximate bandwidth W can be uniquely represented by giving its amplitude and phase at ΘW equally spaced intervals in time or frequency.

Rice has shown that for Gaussian signals the coefficients a_i and b_i have Rayleigh probability distributions. That is,

$$p(a_i) = \frac{2a_i}{\overline{a_i^2}} \exp\left(\frac{-a_i^2}{\overline{a_i^2}}\right) \tag{7}$$

$$p(b_i) = \frac{2b_i}{\overline{b_i^2}} \exp\left(\frac{-a_i^2}{\overline{a_i^2}}\right)$$

where the overscore indicates an average over the ensemble of functions of duration Θ. The average of a_i^2 over the ensemble is given by

$$\overline{a_i^2} = 2\, S(\omega_i)\, \Delta\omega$$

where $S(\omega)$ is the single-sided power spectrum of s(t). The average value of a_i^4 over the ensemble is given by

$$\overline{a_i^4} = \int_0^\infty a_i^4\, p(a_i)\, da_i = \int_0^\infty a_i^4 \frac{2a_i}{\overline{a_i^2}} \exp\left(-\frac{a_i^2}{\overline{a_i^2}}\right) da_i \tag{8}$$

Integration by parts yields

$$\begin{aligned}\overline{a_i^4} &= 2\overline{a_i^2} \int_0^\infty a_i^2 \frac{2a_i}{\overline{a_i^2}} \exp\left(\frac{-a_i^2}{\overline{a_i^2}}\right) da_i \\ &= 2\,\overline{a_i^2} \cdot \overline{a_i^2} = 2\left(\overline{a_i}\right)^2 \\ &= 8\, S^2(\omega_i)(\Delta\omega)^2\end{aligned} \tag{9}$$

Similarly

$$\overline{b_i^2} = 2N(\omega_i)\,\Delta\omega \tag{10}$$

$$\overline{b_i^4} = 8\, N^2(\omega_i)(\Delta\omega)^2 \tag{11}$$

Equations (5) and (6) are used later in the analysis.

The output of the MARK multiplier is

$$s(t)\left[s(t) + n(t)\right] = s^2(t) + s(t)\,n(t) \tag{12}$$

In terms of the Fourier expansions this becomes

$$\left[\sum_{i=1}^{\theta W} a_i \cos(\omega_i t+\phi_i)\right]^2 + \sum_{i=1}^{\theta W} a_i \cos(\omega_i t+\phi_i) \sum_{i=1}^{\theta W} b_i \cos(\omega_i t+\nu_i) \qquad (13)$$

$$\equiv \quad V_I(\omega_i) \quad + \quad V_{II}(\omega_i)$$

The dc component of V_I is seen to be $V_I(0) = \sum_{i=1}^{\theta W} a_1^2$. The corresponding dc power is

$$P_I(0) = V_I^2(0) = \frac{1}{4}\sum_{i=1}^{\theta W} a_i^4 + \frac{1}{4}\sum_{i=1}^{\theta W} a_i^2 \sum_{i\neq j} a_j^2 \qquad (14)$$

The average value of $P_I(0)$ is found by averaging over the ensemble of time functions.

$$\overline{P_I(0)} = \frac{1}{4}\sum_{i=1}^{\theta W} \overline{a_i^4} + \frac{1}{4}\sum_{i=1}^{\theta W} \overline{a_i^2} \sum_{i\neq j} \overline{a_j^2} \qquad (15)$$

At frequencies other than zero $\omega_i = 2\pi n/\theta$, where $n = 1,2,3,\cdots\theta W$ it follows that

$$\begin{aligned} V_I(\omega) \equiv V_I\left(\tfrac{2\pi n}{\theta}\right) &= \frac{1}{2}\sum_i a_i a_{i+n} \cos\left(\tfrac{2\pi nt}{\theta} + \phi_{i+n} - \phi_i\right) \\ &\quad + \frac{1}{2}\sum_i a_{i+n} a_i \cos\left(\tfrac{2\pi nt}{\theta} + \phi_{i+n} - \phi_i\right) \\ &= \sum_i a_i a_{i+n} \cos\left(\tfrac{2\pi nt}{\theta} + \phi_{i+n} - \phi_i\right) \\ &= \cos\tfrac{2\pi nt}{\theta}\sum_i a_i a_{i+n} \cos(\phi_{i+n}-\phi_i) - \sin\tfrac{2\pi nt}{\theta}\sum_i a_i a_{i+n} \sin(\phi_{i+n}-\phi_i) \end{aligned} \qquad (16)$$

The corresponding power is

$$P_I\left(\frac{2\pi n}{\Theta}\right) = \frac{1}{2} V_I^2\left(\frac{2\pi n}{\Theta}\right)$$

$$= \frac{1}{2}\sum_i \left[a_i a_{i+n} \cos(\phi_{i+n} - \phi_i)\right]^2 + \frac{1}{2}\sum_i \left[a_i a_{i+n} \sin(\phi_{i+n} - \phi_i)\right]^2$$

$$+ \Big[\text{terms involving products of the form } \sin\phi_j \sin\phi_k \text{ or } \cos\phi_j \cos\phi_k,\ j \neq k\Big] \qquad (17)$$

The ensemble average of these last terms is zero since the phases ϕ_i are randomly distributed in the interval 0 to 2π. It follows that

$$\overline{P_I\left(\frac{2\pi n}{\Theta}\right)} = \frac{1}{2}\sum \overline{a_i^2}\ \overline{a_{i+n}^2} \qquad n \neq 0 \qquad (18)$$

The component of V_{II} at zero frequency is found as

$$V_{II}(0) = \frac{1}{2}\sum_i a_i b_i \cos(\phi_i - \nu_i) \qquad (19)$$

$$\overline{P_{II}(0)} = \frac{1}{4}\sum_i \overline{a_i^2}\ \overline{b_i^2}\ \overline{\cos^2(\phi_i - \nu_i)}$$

$$+ \frac{1}{4}\sum_i \bar{a}_i \bar{b}_i\ \overline{\cos(\phi_i - \nu_i)} \sum_{i \neq j} \bar{a}_i \bar{b}_i\ \overline{\cos(\phi_j - \nu_j)} \qquad (20)$$

However, $\overline{\cos(\phi_i - \nu_i)} = 0$ since ϕ and ν are independent. Therefore

$$P_{II}(0) = \frac{1}{8} \sum_i \overline{a_i^2}\ \overline{b_i^2} \tag{21}$$

At frequencies different from zero

$$V_{II}\left(\frac{2\pi n}{\theta}\right) = \frac{1}{2}\left[\sum_i a_i b_{i+n} \cos\left(\frac{2\pi n t}{\theta} + \phi_{i+n} - \nu_i\right) + \sum_i a_{i+n} b_i \cos\left(\frac{2\pi n t}{\theta} - \phi_i + \nu_{i+n}\right)\right] \tag{22}$$

By following a procedure similar to that for $V_I(\frac{2\pi n}{\theta})$ it can be shown that

$$P_{II}\left(\frac{2\pi n}{\theta}\right) = \frac{1}{8} \sum_i \left(\overline{a_i^2}\,\overline{b_{i+n}^2} + \overline{a_{i+n}^2}\,\overline{b_i^2}\right) \tag{23}$$

The line spectra of the multiplier output has now been found. To obtain the spectra at the output of the integrator, the above must be multiplied by the power frequency response of the integrator $|I(\omega)|^2$. Also, θ is allowed to become infinite in such a way that the summations become integrals.

Taking first the signal component, $P_I(0)$, the output signal power becomes

$$S_{01} = \lim_{\theta \to \infty} |I(0)|^2 \left(\frac{1}{4} \sum_i \overline{a_i^4} + \frac{1}{4} \sum_i \overline{a_i^2} \sum_{i \neq j} \overline{a_j^2} \right)$$

$$= \lim_{\substack{\theta \to \infty \\ \Delta\omega = \frac{2\pi}{\theta}}} |I(0)|^2 \left[2 \sum_i S^2(\omega_i)(\Delta\omega_i)^2 + \sum_i S(\omega_i)\Delta\omega \sum_{i \neq j} S(\omega_j)\Delta\omega \right]$$

$$= |I(0)|^2 \left[2(0) + \int_0^\infty S(\omega)\, d\omega \int_0^\infty S(\xi)\, d\xi \right]$$

$$= |I(0)|^2 \left[\int_0^\infty S(\omega)\, d\omega \right]^2 \qquad (24)$$

The summation of the remaining components $P_I(\frac{2\pi n}{\theta})$, $P_{II}(0)$, and $P_{II}(\frac{2\pi n}{\theta})$ represents the output fluctuation power or noise, N_{01}, given by

$$N_{01} = \lim_{\theta \to \infty} \sum_{n=0}^{\infty} |I(\tfrac{2\pi n}{\theta})|^2 \left\{ \frac{1}{2} \sum_i 4 S(\xi) S(\xi+\omega)\, \Delta\xi\, \Delta\omega \right.$$
$$\left. + \frac{1}{8} \sum_i \left[4S(\xi)N(\xi+\omega) + 4S(\xi+\omega)N(\xi) \right] \Delta\xi\, \Delta\omega \right\}$$
$$= \int_0^\infty |I(\omega)|^2 \left\{ \int_0^\infty \left[2S(\xi)S(\xi+\omega) + \frac{1}{2} S(\xi)N(\xi+\omega) \right.\right.$$
$$\left.\left. + \frac{1}{2} S(\xi+\omega)N(\omega) \right] d\xi \right\} d\omega \qquad (25)$$

In most cases of practical interest it may be assumed that the power transfer function of the integrator $|I(\omega)|^2$ is quite narrow compared to the width of the input spectra. Further, the spectra of the input signals may be assumed

to be reasonably continuous. Under these assumptions the spectrum of the multiplier output does not vary appreciably over the bandwidth of the integrator. Consequently, the above expressions for S_{01} and N_{01} may be simplified somewhat, thereby becoming

$$S_{01} = |I(0)|^2 \left[\int_0^\infty S(\omega)\, d\omega\right]^2 \tag{26}$$

$$N_{01} = \int_0^\infty |I(\omega)|^2 d\omega \int_0^\infty \left[2S^2(\omega) + S(\omega)N(\omega)\right] d\omega \tag{27}$$

The signal-to-noise ratio at the output of the MARK filter is

$$\frac{S_{01}}{N_{01}} = \frac{|I(0)|^2}{\int_0^\infty |I(\omega)|^2 d\omega} \quad \frac{\left[\int_0^\infty S(\omega)\, d\omega\right]^2}{\int_0^\infty \left[2S^2(\omega) + S(\omega)N(\omega)\right] d\omega} \tag{28}$$

The factor $\frac{|I(0)|^2}{\int_0^\infty |I(\omega)|^2 d\omega} \equiv \frac{1}{W_i}$ is the reciprocal of the effective bandwidth of the integrator.

III. CALCULATION OF THE TRANSFER FUNCTION AND EFFECTIVE BANDWIDTH OF THE INTEGRATOR

An ideal integrator, if turned on at time t = 0 and reset at t = T would have an impulse response

$$i(t) = \begin{cases} 1, & 0<t<T \\ 0, & t<0 \text{ or } T<t \end{cases} \tag{29}$$

The integrator transfer function $I(\omega)$ is found by taking the Fourier transform of the impulse response.

$$I(\omega) = \int_{-\infty}^{\infty} i(t)\, e^{-j\omega t}\, dt = \int_{0}^{T} 1 \cdot e^{-j\omega t}\, dt$$

$$= \frac{1 - e^{-j\omega T}}{j\omega} = \frac{-\sin \omega T}{\omega} - j\left(\frac{1-\cos \omega T}{\omega}\right) \tag{30}$$

The square of the magnitude of $I(\omega)$ is

$$|I(\omega)|^2 = T^2 \frac{\sin^2\left(\frac{\omega T}{2}\right)}{\left(\frac{\omega T}{2}\right)^2} \tag{31}$$

And finally, the integral of the magnitude-squared over all positive frequencies is found as

$$\int_0^{\infty} |I(\omega)|^2 d\omega = 2T \int_0^{\infty} \frac{\sin^2\left(\frac{\omega T}{2}\right)}{\left(\frac{\omega T}{2}\right)^2}\, d\left(\frac{\omega T}{2}\right) = \pi T \tag{32}$$

The effective bandwidth W_1 of the integrator is

$$W_i = \frac{\int_0^\infty |I(\omega)|^2 d\omega}{|I(0)|^2} = \frac{\pi T}{T^2} = \frac{\pi}{T} \tag{33}$$

IV. CALCULATION OF THE OUTPUT NOISE OF THE SPACE CORRELATOR

The noise power at the output of the SPACE integrator is found from Equation (27), noting that the MARK signal appears as noise to the SPACE correlator. The first term of the integrand of (27) disappears, while $N(\omega)$ is replaced by $N(\omega) + S(\omega)$ since the MARK signal is incoherent with the reference input to the SPACE correlator. The resulting expression for the output noise of the SPACE correlator is

$$N_{02} = \int_0^\infty |I(\omega)|^2 d\omega \int_0^\infty S(\omega)\left[S(\omega) + N(\omega)\right] d\omega \tag{34}$$

where the subscript 2 is used to indicate that the quantity pertains to the SPACE correlator. Rewriting equations (26), (27), and (34) in terms of power densities per radian

$$S_{01} = S_i^2 |I(0)|^2 \left[\int_0^\infty H(\omega)\, d\omega\right]^2 \tag{35}$$

$$N_{01} = \left(2 S_i^2 + S_i N_i\right) \int_0^\infty |I(\omega)|^2 d\omega \int_0^\infty H^2(\omega)\, d\omega \tag{36}$$

$$N_{02} = \left(S_i^2 + S_i N_i\right) \int_0^\infty |I(\omega)|^2 d\omega \int_0^\infty H^2(\omega)\, d\omega \tag{37}$$

V. DERIVATION OF THE PROBABILITY OF ERROR

The probability distribution of the voltages corresponding to N_{01} and N_{02} are Gaussian. To show this it is necessary to recall that before θ was allowed to become infinite in the derivation of these terms the amplitude of each frequency component was the product of two statistically independent, random quantities. The phase of each component of the product was also random and independent of the phase of the other components. By the central limit theorem the sum of a large number of independent random components must approach a Gaussian process as the number of components increases without bound, regardless of the statistics of the individual components. The mean of the sum is zero in the present case since the phase of the components is uniformly distributed in the interval $0<\theta<2\pi$.

Let x_1 and x_2 represent the output voltages of the MARK and SPACE correlators respectively at the end of an integration period. The probability distributions of x_1 and x_2 may be written

$$p(x_1) = \frac{1}{\sqrt{2\pi N_{01}}} \exp\left[\frac{-(x_1-\sqrt{S_{01}})^2}{2N_{01}}\right] \tag{38}$$

$$p(x_2) = \frac{1}{\sqrt{2\pi N_{02}}} \exp\left[\frac{-x_2^2}{2N_{02}}\right] \tag{39}$$

It should be remembered that x_1 represents the sum of the signal and noise at the output of the MARK correlator.

An incorrect decision is made whenever x_2 exceeds x_1. This is equivalent to x_1-x_2 being negative. To calculate the probability of error it is convenient to first determine the probability distribution of $x \equiv x_1-x_2$. Since x_1 and x_2 are independent Gaussian variates, their difference is also a Gaussian variate with mean and variance equal to the sum of the means and variances, respectively, of x_1 and x_2.

$$p(x) = \frac{1}{\sqrt{2\pi(N_{01}+N_{02})}} \quad \exp\left[\frac{-(x-\sqrt{S_{01}})^2}{2(N_{01}+N_{02})}\right] \tag{40}$$

The probability of error P_e is found by integrating $p(x)$ over all negative values of x.

$$P_e = \frac{1}{\sqrt{2\pi(N_{01}+N_{02})}} \int_{-\infty}^{0} \exp\left[\frac{-(x-\sqrt{S_{01}})^2}{2(N_{01}+N_{02})}\right] dx \tag{41}$$

$$\text{let} \quad y = \frac{-x+\sqrt{S_{02}}}{\sqrt{2(N_{01}+N_{02})}} \qquad dy = \frac{-dx}{\sqrt{2(N_{01}+N_{02})}}$$

$$P_e = \frac{1}{\sqrt{\pi}} \int_{\sqrt{\frac{S_{01}}{2(N_{01}+N_{02}}}}^{\infty} \exp(-y^2) \quad dy$$

$$P_e = \frac{1}{2}\left[1 - \operatorname{erf}\sqrt{\frac{S_{01}}{2(N_{01}+N_{02})}}\right] \tag{42}$$

VI. NUMERICAL EVALUATION OF PROBABILITY OF ERROR

The probability of error was found to be a function of

$$E \equiv \sqrt{\frac{S_{01}}{2(N_{01}+N_{02})}}$$

Upon substitution of Equations (30), (31), and (32) into the above, and after some manipulation

$$E = \sqrt{\left\{\frac{\left[\int_0^\infty H(\omega)\,d\omega\right]^2}{\int_0^\infty H^2(\omega)\,d\omega} \cdot \frac{|I(0)|^2}{\int_0^\infty |I(\omega)|^2 d\omega}\right\} \frac{S_i/N_i}{6\frac{S_i}{N_i}+4}} \tag{43}$$

The term in braces, which represents a system constant, is next calculated.

Numerical integration of $H(\omega)$ and $H^2(\omega)$ as indicated in the appendix yields

$$\int_0^\infty H(\omega)\,d\omega = 32,600 \tag{44}$$

$$\int_0^\infty H^2(\omega)\,d\omega = 26,700 \tag{45}$$

Substitution for T in Equation (33) gives

$$\frac{1}{W_i} = \frac{.0333}{\pi} = .01061 \tag{46}$$

And, upon substitution of these values into Equation (38), it is found that

$$E = \sqrt{2\ln\frac{S_i/N_i}{3S_i/N_i + 2}} \tag{47}$$

Using published tables of the error function[7], numerical values of P_e were calculated as a function of S_i/N_i. The results of these calculations are presented in Table I and Figure 3.

TABLE I

CALCULATED VALUES OF PROBABILITY OF ERROR

S_i/N_i (db)	S_i/N_i	E	P_e
-8	.158	3.68	9.74×10^{-8}
-9	.126	3.34	1.16×10^{-6}
-10	.100	3.03	9.13×10^{-6}
-11	.0795	2.74	5.33×10^{-5}
-12	.0631	2.46	2.52×10^{-4}
-13	.0501	2.22	8.46×10^{-4}
-14	.0398	1.98	2.55×10^{-3}
-15	.0316	1.78	5.91×10^{-3}
-16	.0251	1.600	1.18×10^{-2}
-17	.0199	1.43	2.16×10^{-2}
-18	.0158	1.28	3.55×10^{-2}
-19	.0126	1.14	5.32×10^{-2}
-20	.0100	1.02	7.46×10^{-2}

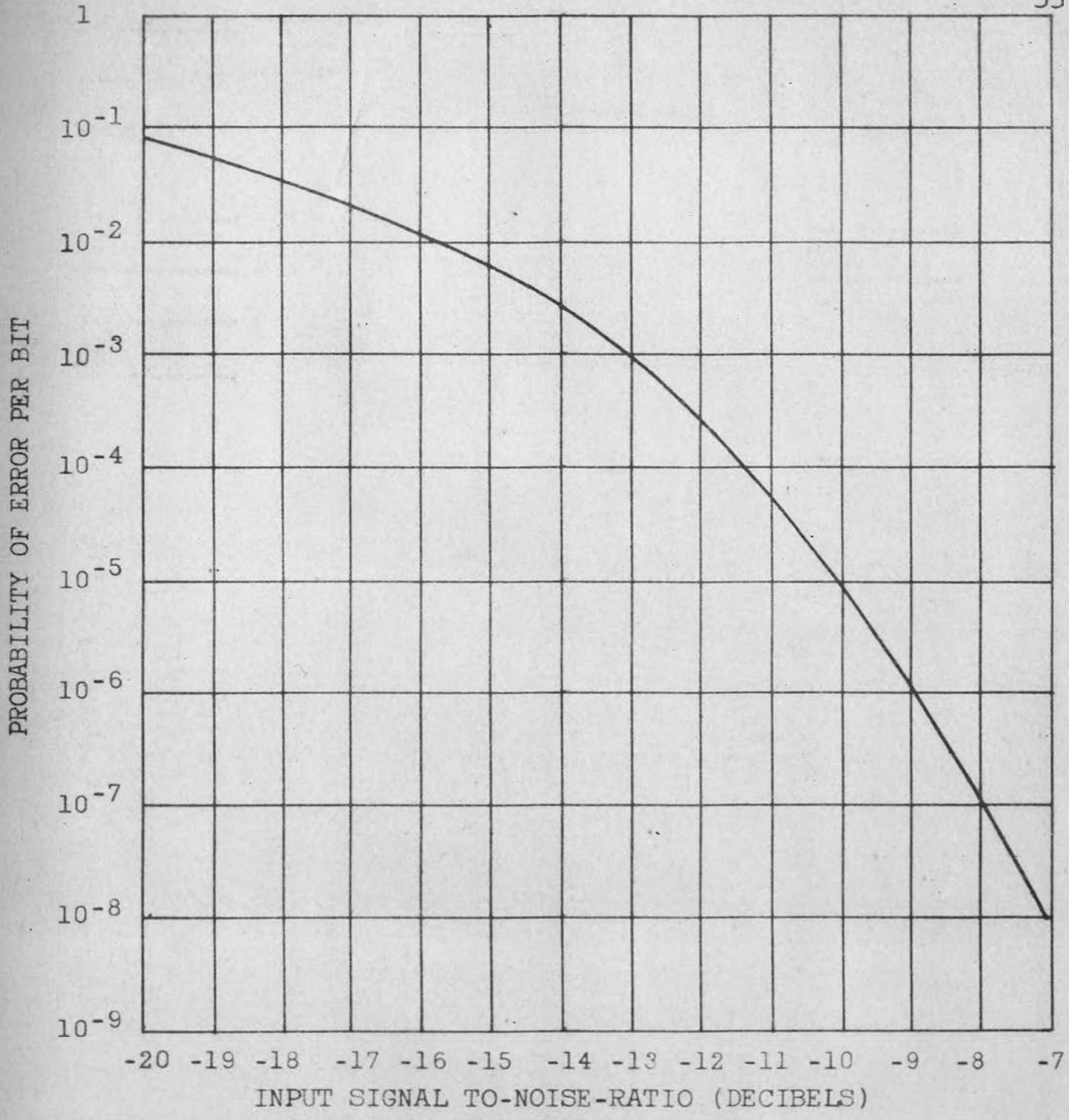

FIGURE 3

PROBABILITY OF ERROR VERSUS INPUT SIGNAL-TO-NOISE RATIO

CHAPTER V

DEVELOPMENT OF THE EXPERIMENTAL EQUIPMENT

The development of the experimental equipment involved two phases. The first phase consisted of finding a system which would adequately simulate the operation of a cross-correlation communication system and yet not be prohibitively complex nor expensive. The second phase consisted of designing the individual components of the system and constructing the equipment.

I. SYSTEM DESIGN

Figure 4 depicts the functional form of the experimental equipment. The following simplifications, designed to minimize the complexity of the equipment, are in evidence:

1. The correlator reference signals were not generated at the receiver, but were obtained from the transmitter signal sources.
2. The transmitted "message" consisted simply of alternate MARK and SPACE symbols.
3. The digital circuitry was common to transmitter and receiver.

Physically, the system consisted of one chassis and

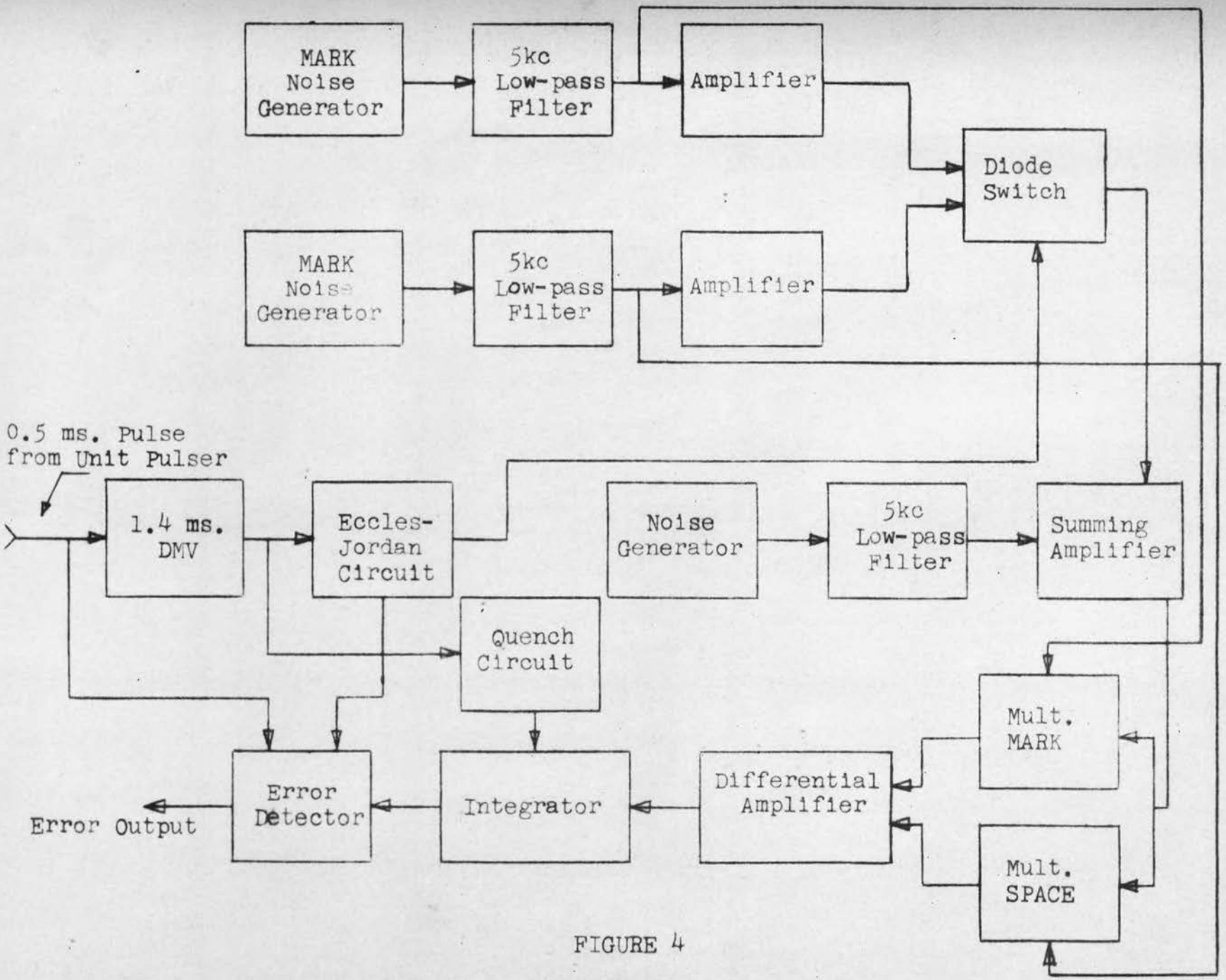

FIGURE 4

BLOCK DIAGRAM OF EXPERIMENTAL EQUIPMENT

a Philbrick HKR operational amplifier manifold mounted in a relay rack, as shown in Figure 5. In addition, a General Radio Unit Pulser (system clock) and two laboratory power supplies were used. A modified Berkley Model 1000 Geiger-Muller scaler was used to count errors.

II. COMPONENT DESIGN

Noise Generators. Three physical sources of noise were considered for application as noise generators; resistors, temperature-limited diodes, and gas diodes. The gas diode source was chosen because of its large output noise voltage. The final circuit employed a 6D4 gas triode connected as a diode.

Measurements made using a General Radio Type 736-A wave analyser indicated that the power spectrum of the noise was essentially constant between 30 CPS and 20 KC.

Noise Filters. The purpose of the noise filters was to impart a known shape to the power spectra of the signals and the interference noise. A three-pole Chebyshev design was chosen because it was simple to construct and had a reasonably good rate of attenuation in the stop band. The calculated and measured attenuation characteristics of these filters are plotted in Figure 6. The integrals of

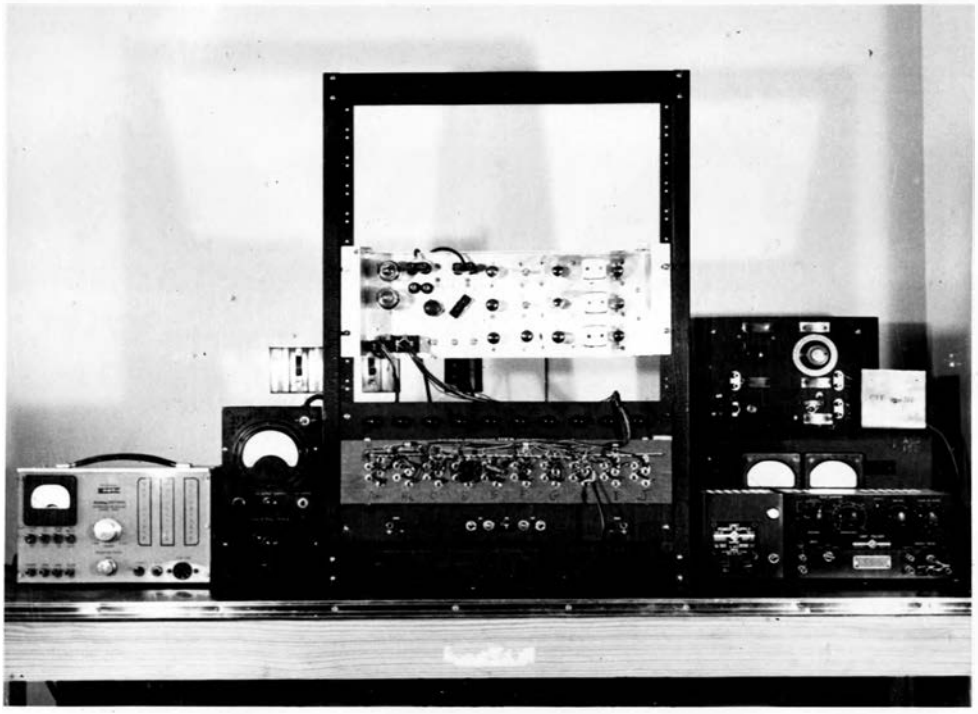

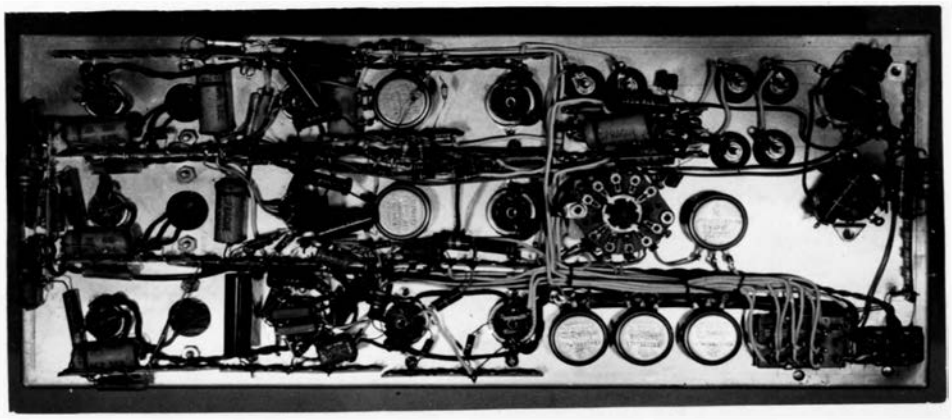

FIGURE 5

EXPERIMENTAL EQUIPMENT

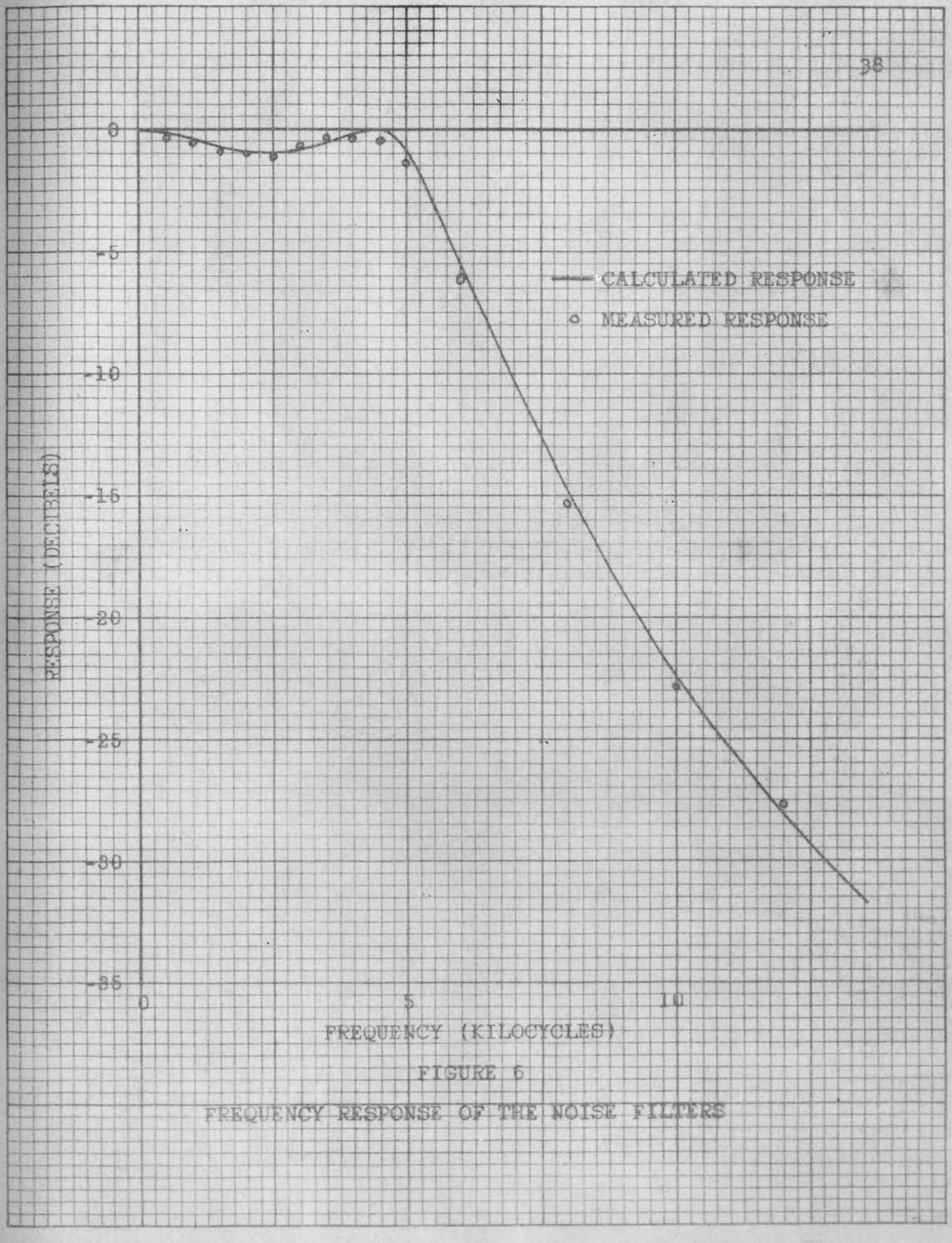

FIGURE 6

FREQUENCY RESPONSE OF THE NOISE FILTERS

$H(\omega)$ and $H^2(\omega)$ are given in the Appendix.

Multiplier. The following specifications were established for the multiplier.

1. Multiplication should be linear for output voltages as much as 20 db greater than the no-signal output noise.
2. The dc. output drift should be small enough that frequent balancing is not required.
3. The bandwidth should exceed 5 kc.
4. The multiplier should be inexpensive and easily constructed.

A review of the literature 8, 9, 10, 11, 12, 13, indicated that multipliers meeting specifications 1, 2 and 3 above were in most cases overly complicated. Two possible exceptions were noted, the varistor ring multiplier and the dual-control vacuum tube multiplier. Of the two, the dual-control vacuum tube circuit appeared to be the most promising.

A type 6AS6 dual control pentode was tentatively selected. Measurements were made to determine over what range of inputs linear multiplication could be obtained. The results of these measurements are shown in Figures 7 and 8. Figure 7 shows output voltage versus control grid

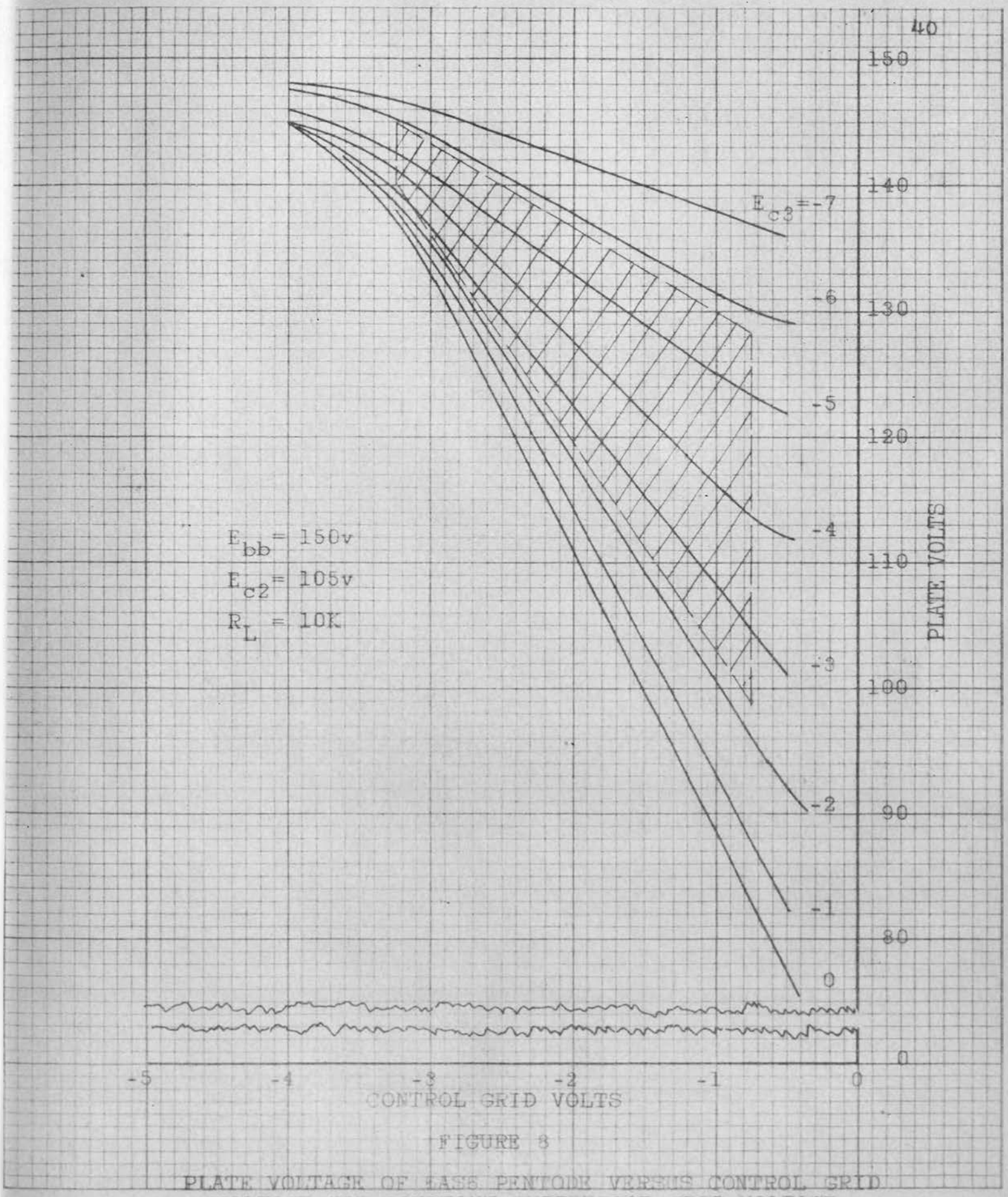

FIGURE 8

PLATE VOLTAGE OF 6A8 PENTODE VERSUS CONTROL GRID VOLTAGE FOR CONSTANT SUPPRESSOR GRID VOLTAGE

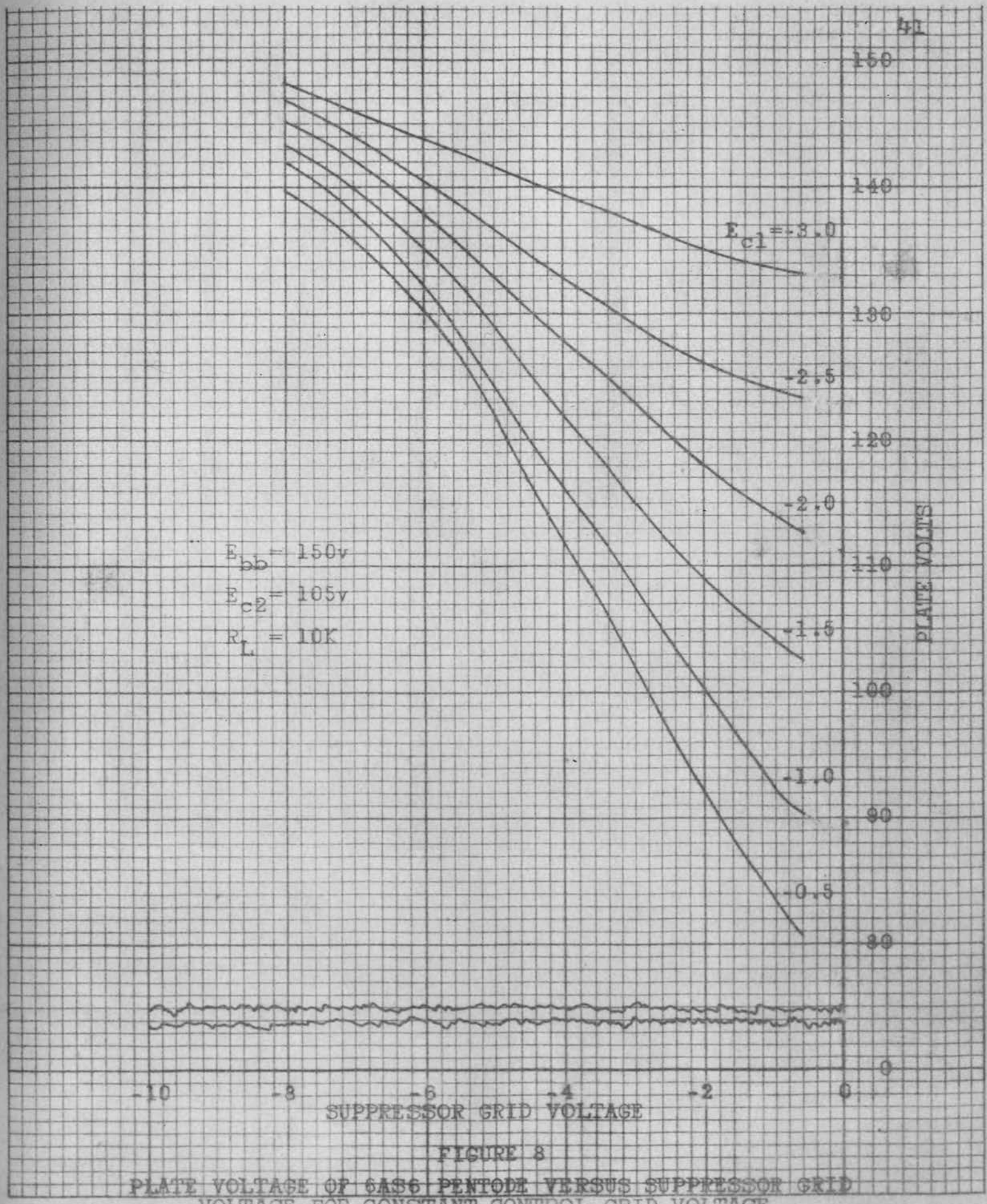

FIGURE 8

PLATE VOLTAGE OF 6AS6 PENTODE VERSUS SUPPRESSOR GRID VOLTAGE FOR CONSTANT CONTROL GRID VOLTAGE

voltage for a series of constant values of suppressor grid voltages. The range of values of control grid voltage for which a proportional output voltage results may be readily determined from this figure. In Figure 8 the same data is represented, but in a form which permits the determination of the linear operating range with respect to suppressor grid voltage. The crosshatched region in Figure 7 defines the range of control grid voltages and suppressor grid voltages in which linear operation results.

The final multiplier circuit is shown in Figure 9. It is seen that the MARK and SPACE multipliers have been combined in such a way that the output is the difference of the two products. This circuit has the advantage that changes of temperature or line voltage cause very little drift of the output. The low drift results from the fact that changes in temperature or line voltage tend to affect both tubes alike, causing the effects to be balanced out.

Integrator. For the integrator, an operational amplifier in the Philbrick HKR operational manifold was used. The circuit for quenching the integrator consists of two triodes connected with their cathodes and plates in anti-parallel across the integrating capacitor. During the integration interval a large negative potential is

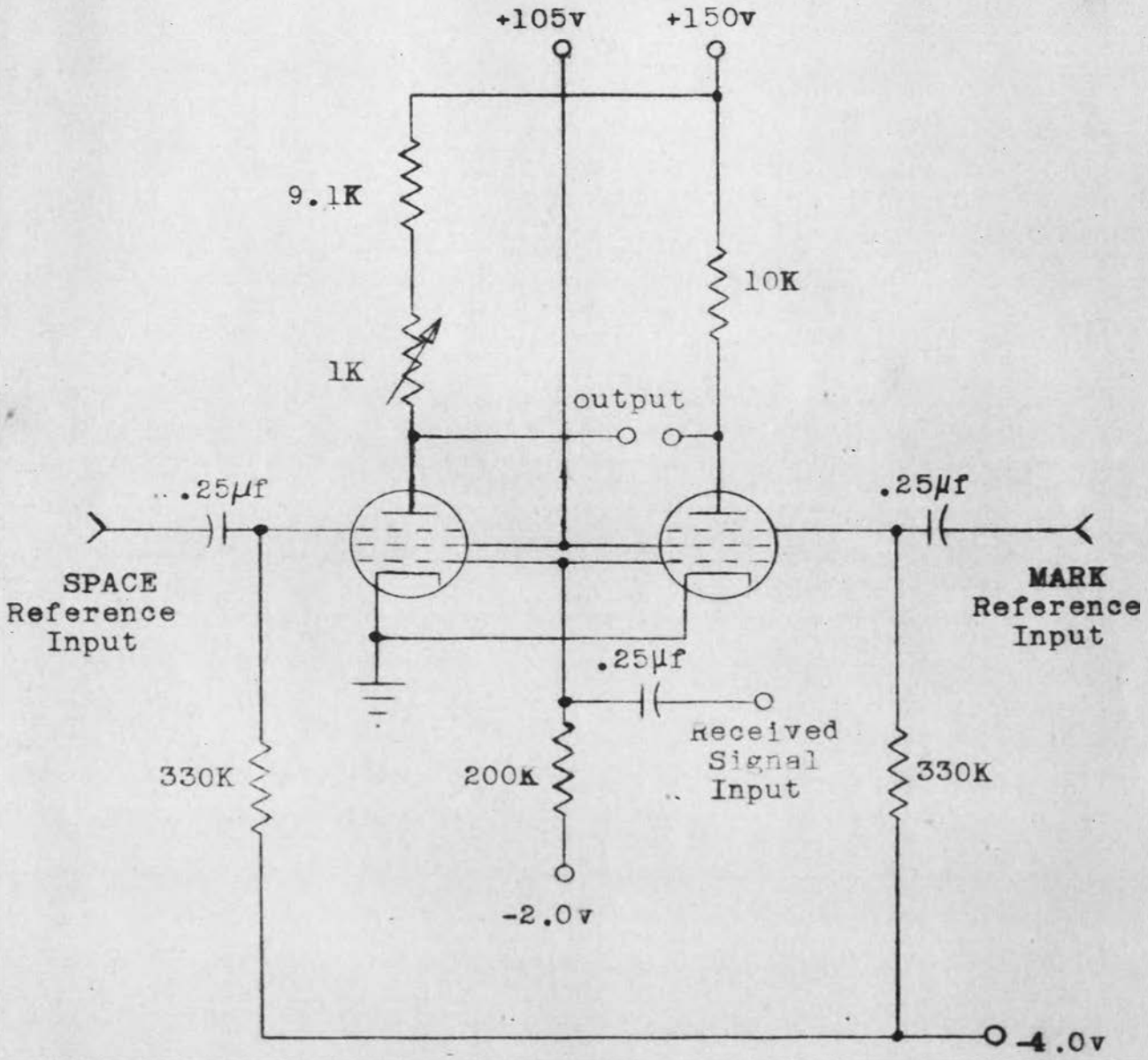

FIGURE 9

ANALOG MULTIPLIER CIRCUIT

applied to their grids. To quench the integrator a positive pulse of 1.4 msec. duration is applied. The time constant of the quench process was found to be 0.1 msec.

Message generator and keyer. An Eccles-Jordan circuit, triggered by the delay multivibrator (DMV) pulse, is used to generate the alternate MARK-SPACE message. The output of the Eccles-Jordan circuit controls a single-pole, double-throw diode switch which in turn selects either MARK or SPACE for transmission.

Error detector. Incorporated in the equipment is a device for automatically detecting errors. It consists of two transistor coincidence-gates which compare the output of the integrator at the sample times with the output of the transmitter message generator. The error detector delivers a pulse to an external counter each time an error is made.

III. OPERATION OF EQUIPMENT

Transmitter. The broad-band noises generated by the three gas tubes are filtered individually by three similar low-pass filters. Two of the filtered noises are used as the MARK and SPACE signals, while the third is used as interference noise. A typical 10 millisecond sample of the

filtered noise is shown in Figure 10. The amplified outputs of the MARK and SPACE filters are applied to corresponding input terminals of the keyer (diode switch). Alternate 33.3 millisecond samples of the two inputs are taken by the keyer in accordance with the input "message" generated by the Eccles-Jordan circuit. Figure 11 shows: (1) the MARK component of the keyed signal, (2) the SPACE component of the keyed signal, and (3) the composite signal. The output of the keyer is considered to be the transmitter output.

Receiver. The transmitted signal, to which interfering noise has been added, is amplified and impressed on the control grids of the multiplier tubes. MARK and SPACE reference signals are applied to the corresponding suppressor grids. Instead of locally generating the reference signals, as would be done in a practical system, they are obtained from the output of the transmitter signal sources.

Next, the difference voltage between the plates of the multiplier tube is integrated. Integration is over a period of 33.3 milliseconds, at the end of which time the integrator is reset to zero. The output of the integrator is amplified and applied to the two, transistor coincidence gates which perform the decision and error detecting operations. In effect these gates compare the polarity of the

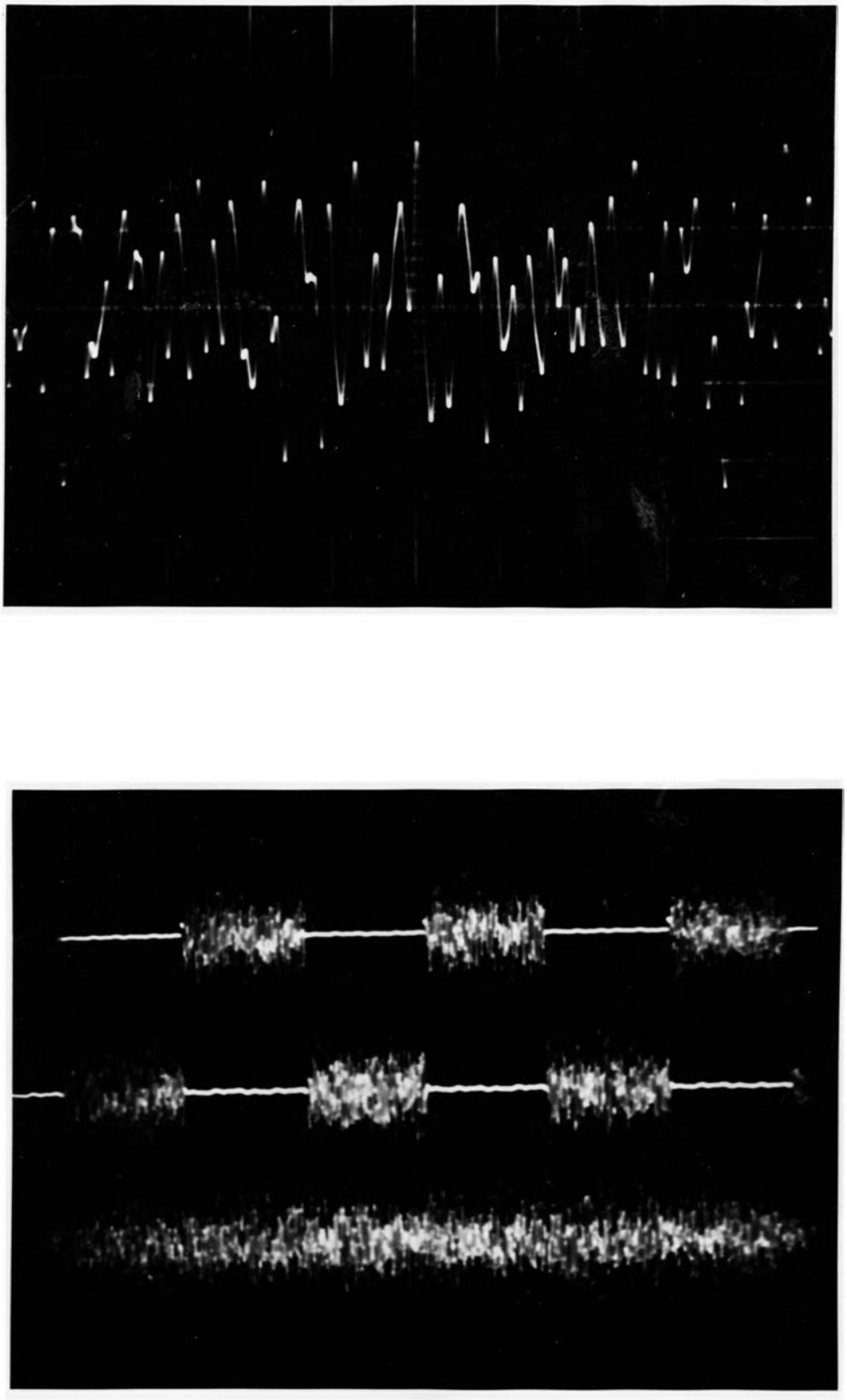

FIGURE 11

TRANSMITTED SIGNAL (1) MARK COMPONENT, (2) SPACE COMPONENT, (3) COMPOSITE SIGNAL

integrator voltage immediately prior to quench with the polarity of the transmitter keying voltage.

Common equipment. The timing and control circuitry is common to both the transmitter and the receiver. A General Radio "Unit Pulser" adjusted to generate 0.5 millisecond pulses with a repetition frequency of 30 cycles per second is used as the system clock. These pulses serve as sampling pulses for the decision circuit of the receiver, and also are used to trigger a 1.4 millisecond delay multivibrator. The delay multivibrator pulse, in turn, serves as the reset pulse for the integrator and triggers the Eccles-Jordan circuit. The time relations between the various signals in the system are illustrated in Figure 12.

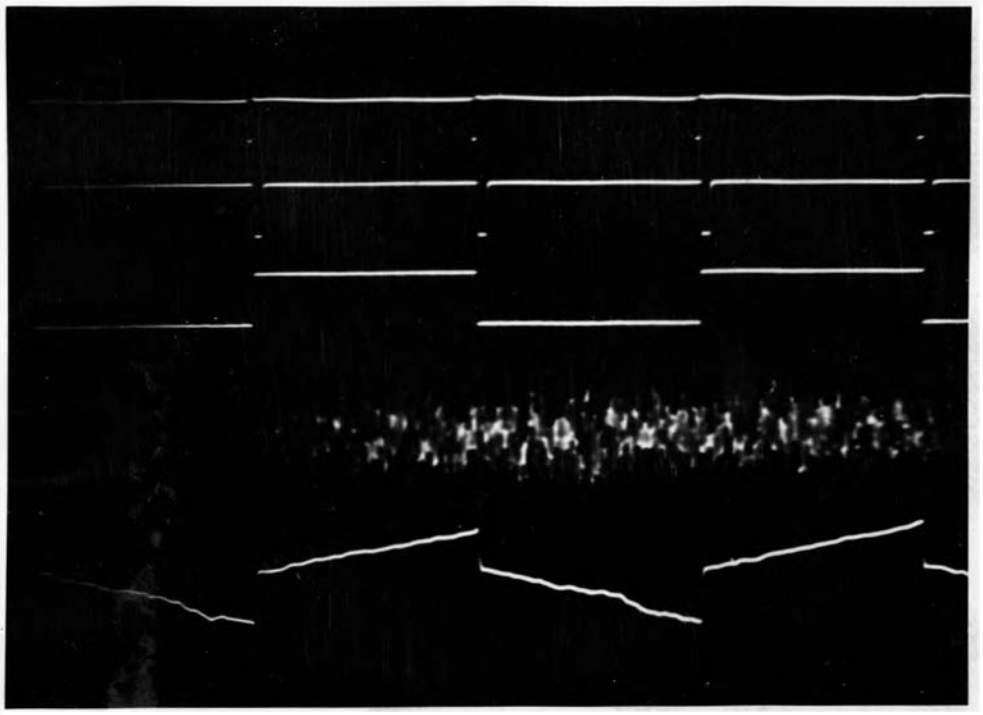

FIGURE 12

TIME RELATIONSHIP OF THE VARIOUS SYSTEM WAVEFORMS
(1) CLOCK PULSE, (2) DMV OUTPUT
(3) TRANSMITTER KEYING SIGNAL
(4) KEYED TRANSMITTER SIGNAL
(5) INTEGRATOR OUTPUT

CHAPTER VI

EXPERIMENTAL INVESTIGATION

Experiments were performed to determine the effect of input signal-to-noise ratio on the probability of error of the experimental equipment. A description of the experimental procedures employed and the results of the experiments are presented in the present chapter.

I. PROCEDURE

Basically, the experiments consisted of adjusting the equipment to obtain various values of input signal-to-noise ratio in the system and counting the number of errors that resulted in a known interval of time. The detailed procedure employed is as follows.

With a Tektronix Model 514AD oscilloscope connected to the suppressor grid of the MARK multiplier tube the gain of the MARK signal source was adjusted until only occasional peaks of the suppressor signal exceeded 3.5 peak to peak volts. This was the peak to peak voltage variation over which multiplication was found to be linear as shown in Figure 8. The signal voltage at the suppressor grid of the MARK multiplier tube was next measured with a Ballantine Model 300 VTVM. The VTVM was then connected to the

suppressor grid of the SPACE multiplier tube, and the gain of the SPACE signal source was adjusted to give the same indication on the VTVM as did the MARK signal. This resulted in the reference inputs to the two multipliers being equal.

With the function switch in the "noise" position the gain of the noise source was adjusted until the peak-to-peak voltage at the control grids of the multiplier exceeded 2.5 volts only occasionally, as indicated by the oscilloscope. Reference to Figure 7 indicates that this is the linear operating range of the multipliers with respect to the control grid voltage. This signal, as measured with the VTVM, was taken to be the input noise level. In operation, the noise voltage was always maintained at this value, and different signal-to-noise-ratios were obtained by adjusting the signal levels. This was accomplished by setting the function switch to either MARK or SPACE and adjusting the common-signal gain control to obtain the desired signal level as indicated by the VTVM.

Before each run the difference amplifier at the output of the multiplier was balanced. This was accomplished by setting the function switch to "noise", shorting out the noise source, and then adjusting the bias control of the amplifier. Balance was indicated by the absence of

a sawtooth waveform at the output of the integrator. A considerable amount of difficulty was experienced with drift in the system. It was found that re-balancing was required at least at five minute intervals. The exact origin of the drift was not determined, but it is believed to be a consequence of the method employed to couple the plates of the multiplier tubes to the input of the difference amplifier.

As a consequence of the drift in the system it was necessary to limit individual runs to two minutes duration. If at the end of the two minutes the amplifiers were out of balance, the data for that run was discarded. The possibility exists, however, that in some runs drift may have occurred during the course of a run but not have been present at the end of the run when the balance was checked.

II. EXPERIMENTAL RESULTS

The results of the tests of the experimental equipment are presented in Table II and Figure 13. It is seen that the experimental points in Figure 13 do not encompass as wide a range of signal-to-noise ratios as does the calculated curve. The reasons for this are two. First, for signal-to-noise ratios greater than 7 db an exorbitant amount of time would have been required to obtain sufficient

TABLE II

PROBABILITY OF ERROR VERSUS INPUT SIGNAL TO NOISE RATIO FOR EXPERIMENTAL EQUIPMENT

S_i/N_i (db)	Total bits	errors	Pe
-12	21,600	237	1.1×10^{-2}
-11	54,000	86	1.6×10^{-3}
-10	108,000	26	2.4×10^{-4}
-9	162,000	19	1.2×10^{-4}

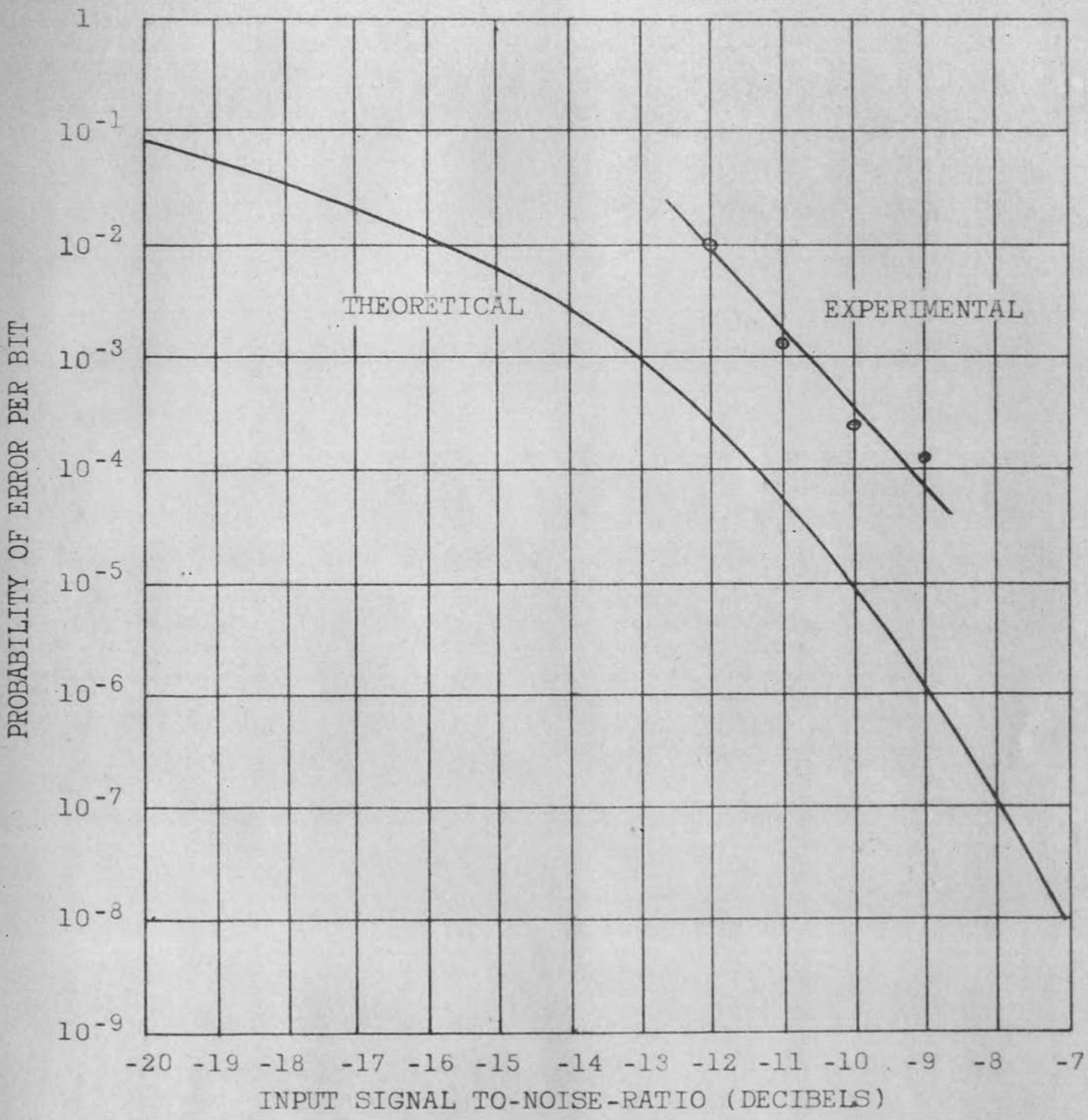

FIGURE 13

PROBABILITY OF ERROR VERSUS INPUT SIGNAL-TO-NOISE RATIO

data. Second, since the maximum noise level was fixed by multiplier linearity considerations the signal-to-noise ratio could be increased only by decreasing the signal level. As the signal was decreased, however, the point was eventually reached where the error rate was determined more by circuit noise and drift than by the noise intentionally introduced.

A pictorial display of the ability of the experimental equipment to operate at low signal-to-noise ratios is shown in Figure 14. The upper oscilloscope trace shows the keyed transmitter signal, while the second trace shows an interfering noise which was 10db greater than the signal. In the third trace the output of the integrator is shown. Comparison of the integrator output with the transmitted "message" (trace 4) indicates that no errors were made during the interval shown.

III. DISCUSSION OF ERRORS

The performance of the experimental equipment appears to be poorer than the predicted performance by an amount which varied from 2.0 db at a probability of error of 10-4, to 3.6 db at a probability of error of 10^{-2}. Several possible reasons for this discrepancy exist. One of these is the fact that the effective integration period used in

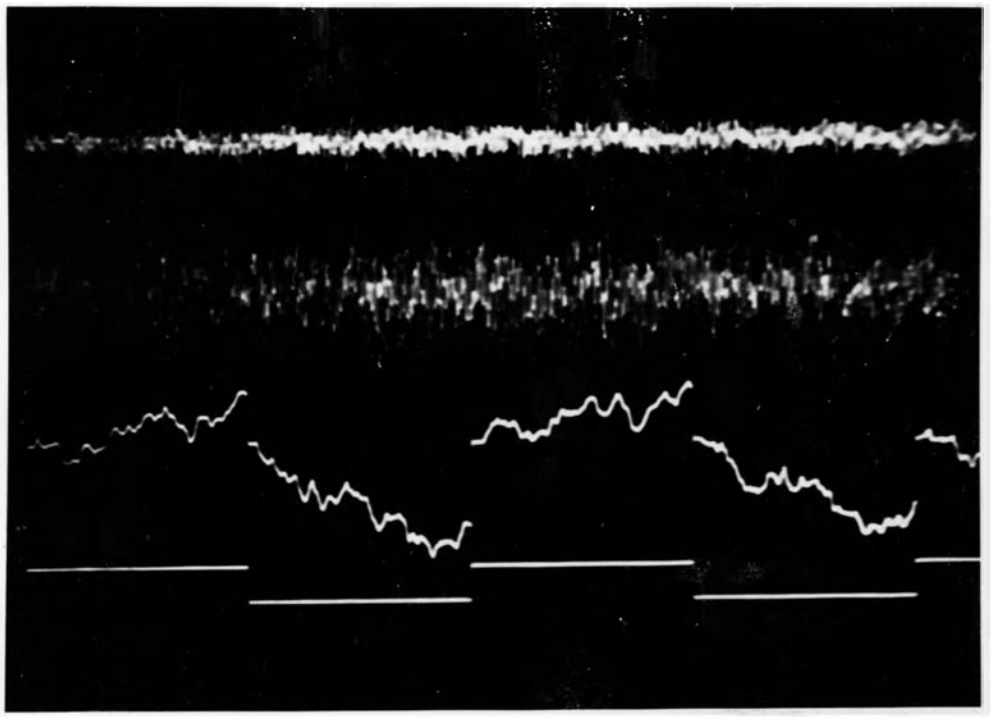

FIGURE 14

DISPLAY OF SYSTEM WAVEFORMS FOR A SIGNAL-TO-NOISE RATIO OF -10 DECIBELS SHOWING (1) KEYED SIGNAL, (2) INTERFERING NOISE, (3) OUTPUT OF THE INTEGRATOR, (4) TRANSMITTER KEYING SIGNAL

the experimental tests was 31.3 milliseconds, whereas the calculations were based on an integration period of 33.3 milliseconds. The 2 millisecond difference represents the time lost in the sample and reset operations. This reduction of integration time accounts for 0.3 db of the difference between the theoretical and the experimental results.

The principal source of error in the experimental results is believed to be the dc drift of the multiplier and difference-amplifier circuitry. Although the amplifier was balanced at the beginning of each run, it appears quite likely that during some runs drift may have occurred of such magnitude as to increase the error rate during those runs.

A third possible source of error lies in the assumption that the various signals and noises employed in the experimental equipment had Gaussian amplitude distributions. A Gaussianly distributed voltage is impossible to realize in practice since it implies the capability of generating and transmitting infinitely large voltage peaks. It is possible that the rather narrow dynamic range of the multiplier may have had a significant effect on the probability distributions of the input signals. Any error resulting from this, however, is believed to be small compared to other sources of error in the experiments.

CHAPTER VII

CONCLUSIONS

The cross-correlation communication system can provide essentially error-free operation at input signal-to-noise ratios considerably less than unity. Such a system employing signals of 5 kilocycle bandwidth and an integration time of 33.3 milliseconds theoretically would make about one error in each 100,000 bits at a signal to noise ratio of -10 db.

For a constant error rate the required input signal to noise ratio is inversely proportional to the product of integration time and signal bandwidth. Improvement of the performance of the system can be achieved, therefore, by increasing either of these parameters. In a given application, however, the available bandwidth and the required information rate are pre-determined, thereby fixing the upper limit of the integration time, bandwidth product.

Although the performance of the experimental equipment was 2 db to 4 db poorer than predicted theoretically, it did serve to verify the fact that a cross-correlation communication system can provide nearly error free service at signal-to-noise ratios less than unity. It is believed that reduction of the considerable dc drift of the system would have resulted in performance more nearly equal to that predicted.

BIBLIOGRAPHY

1. Lee, Y. W., T. P. Cheatham, and J. B. Wiesner, "The Application of Correlation Functions in the Detection of Small Signals in Noise." Technical Report No. 141, Massachusetts Institute of Technology Research Laboratory of Electronics, October 13, 1949.

2. Fano, R. M., "On the Signal-to-Noise Ratio in Correlation Detectors." Technical Report No. 186, Massachusetts Institute of Technology Research Laboratory of Electronics, February 19, 1951.

3. Woodward, P. M. and I. L. Davies, "Information Theory and Inverse Probability in Telecommunication." The Proceedings of the Institution of Electrical Engineers, Vol. 99 (March 1952) pp. 37-44.

4. Green, P. E. "The Output Signal-to-Noise Ratio of Correlation Detectors." I.R.E. Transactions on Information Theory, March 1957, pp. 10-18

5. Goldman, S., Information Theory. New York: Prentice Hall, 1953, pp. 235-243.

6. Rice, S. O., "Mathematical Analysis of Random Noise," Selected Papers on Noise and Stochastic Processes, Edited by Nelson Wax, Dover, 1954, pp. 179-181.

7. Federal Works Agency Work Projects Administration for the City of New York, Tables of Probability Functions, Vol. I (Washington: Government Printing Office, 1941).

8. Somerville, M. J., "An Electronic Multiplier." Electronic Engineering, Vol. 24 (February 1952), pp. 78-80

9. Mehron, M., "Instantaneous Multiplier for Computers." Electronics, Vol. 27 (February 1954), pp. 144-148.

10. Garrett, D. E., "A General Purpose Electronic Voltmeter." Proceedings of the Institute of Radio Engineers, Vol. 40 (February 1952), pp. 165-171.

11. El-Said, M. A. H., "Novel Multiplier Circuits." Proceedings of the Institute of Radio Engineers, Vol. 37 (September 1949), pp. 1003-1015.

12. Sydnor, R. L., T. R. O'Meara, J. Strathman, "Analog Multipliers and Squarers Using a Multigrid Modulator," I.R.E. Transactions on Electronic Computers, June 1956, pp. 82-85.

13. Chance, B., and others, Waveforms. Vol. XIX of MIT Radiation Series. New York: McGraw-Hill, 1949, pp. 667-693.

APPENDIX. CALCULATION OF $\int_0^\infty H(\omega)d\omega$ AND $\int_0^\infty H^2(\omega)\ d\omega$

The square of the magnitude of the transfer function of a 3-pole, 1 decibel-ripple, Chebyshev low pass filter with a tolerance bandwidth of W radians per second may be written

$$H(\omega) = \frac{1}{1 + .26\ C_3^2\left(\frac{\omega}{W}\right)}$$

where C_3 is the 3rd order Chebyshev polynomial, $C_3(x) = 4x^3-3x$.

The integrals of $H(\omega)$ and $H^2(\omega)$ can be evaluated analytically by expanding the integrand in partial fractions. However, a numerical procedure would be required to evaluate the poles of $H(\omega)$ and $H^2(\omega)$. It was decided, therefore, to evaluate the integrals themselves by numerical methods. For these calculations, Simpson's rule was used with an interval of 1 kilocycle (6280 radians). Simpson's rule for even n may be written.

$$\int_a^b f(x)\,dx \approx \frac{h}{3}\left(f_0 + 4f_1 + 2f_2 + 4f_3 + \cdots + 4f_{n-1} + f_n\right)$$

where h is equal to $|b-a|/n$. The numerical calculations performed in evaluating the integrals, and the results obtained are shown in Table III.

TABLE III

NUMERICAL INTEGRATION OF $H(\omega)$ AND $H^2(\omega)$

f(KC)	H(f)	Simpson's coefficient	$H^2(f)$	Simpson's coefficient
0	1.00	1.00	1.00	1.00
1	.92	3.68	.845	3.38
2	.83	1.66	.688	1.38
3	.83	3.32	.688	2.75
4	.87	1.74	.756	1.51
5	.81	3.24	.655	2.62
6	.25	.50	.062	.12
7	.088	.35	.008	.03
8	.025	.05	.001	.00
9	.012	.05	.000	.00
10	.0055	.00	.000	.00
11	.0025	.00	.000	.00
12	.0017	.00	.000	.00
		15.61		12.79

$$\int_0^\infty H(f)df \approx \frac{1000}{3}(15.61) = 5200 \text{ watt-cycles} = 32{,}600 \text{ watt-radians}$$

$$\int_0^\infty H^2(f)df \approx \frac{1000}{3}(12.79) = 4260 \text{ watt}^2\text{-cycles} = 26{,}700 \text{ watt}^2\text{-radians}$$

Note:
All Diodes IN297
Transistors are college left rejects of unknown types
Capacitance values larger than unity are microfarads. Values less than unity are microfarads

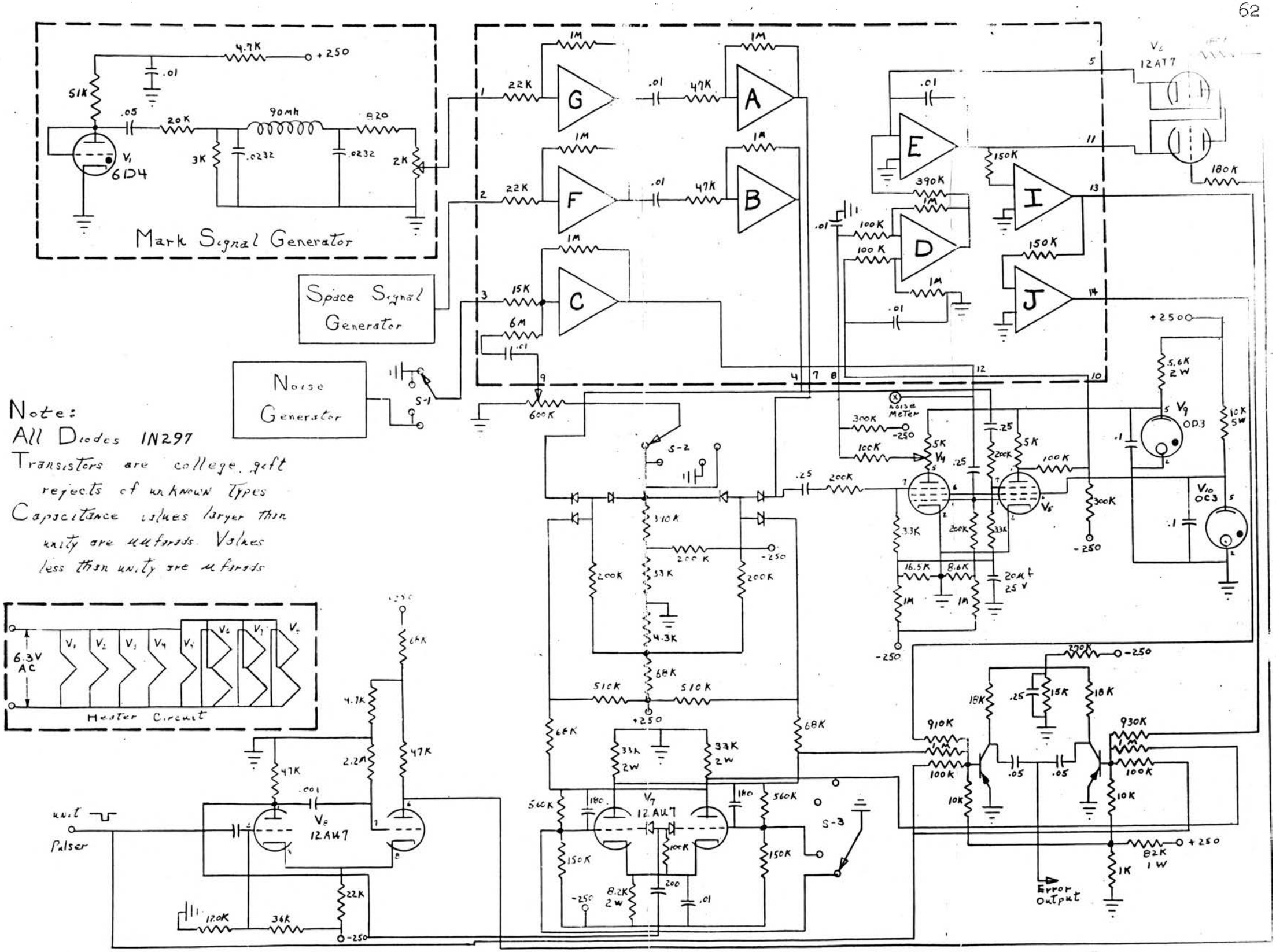

FIGURE 15 EXPERIMENTAL CROSS-CORRELATION COMMUNICATION SYSTEM

VITA

Dennis J. Gooding was born on June 24, 1933, near Verona, Missouri. He attended public schools in Vandalia, Illinois; Verona, Missouri; Evansville, Indiana; Upland, California; Cucamonga, California; and Pasadena, California. He was graduated from Verona High School in 1951.

Upon graduation from high school, the author entered Southwest Missouri State College where he pursued a pre-engineering curriculum. In September, 1953 he transferred to the Missouri School of Mines and Metallurgy, from which he was graduated in May, 1956, with the degree of Bachelor of Science in Electrical Engineering. He was employed as a student assistant in the Department of Electrical Engineering from February, 1955 until graduation.

The author accepted a position with the Stromberg-Carlson Company of Rochester, New York in June, 1956. He was employed in the Research and Advanced Development Department, where he was engaged in research and development work and system studies of data transmission systems.

In September, 1958, he began graduate studies at the Missouri School of Mines and Metallurgy, and accepted a graduate assistantship.

The author returned to Stromberg-Carlson Company for the summer of 1959.

He is a member of the Institute of Radio Engineers, Eta Kappa Nu, and Tau Beta Pi.